Woods et al., *Headphone screening to facilitate web-based auditory experiments*

Supplemental Material

Acoustical modeling of interference effects

The headphone screening task requires that the 0°/180° (anti-phase) tone is attenuated by more than 6dB at the participant's ears when broadcast over stereo loudspeakers – this will ensure it is the lowest-level signal in the discrimination task. The exact attenuation induced by interference varies with specific details of the listener's environment, such as the location and model of the loudspeakers (they may be external or inside a laptop), the exact location of the participant's head, and room reverberation. Here we consider the expected effect of variations in such parameters and demonstrate that a 0°/180° phase difference will typically result in considerable free-field attenuation. This phase-induced attenuation can be easily derived for the simple case of speakers that broadcast uniformly into space (Fig. S1A-B), and we demonstrate that the predicted attenuation is sufficient for the screening task provided that the signal frequency is low. We show that the reverberant energy in an enclosed room is also attenuated by a 0°/180 phase shift because the speakers are less efficient at radiating energy for anti-phase signals. Finally, we show a few examples to demonstrate that the large-scale structure of the attenuation is preserved in more complicated scenes with non-uniform speakers and with reflections from nearby surfaces (Fig. S1C-D).

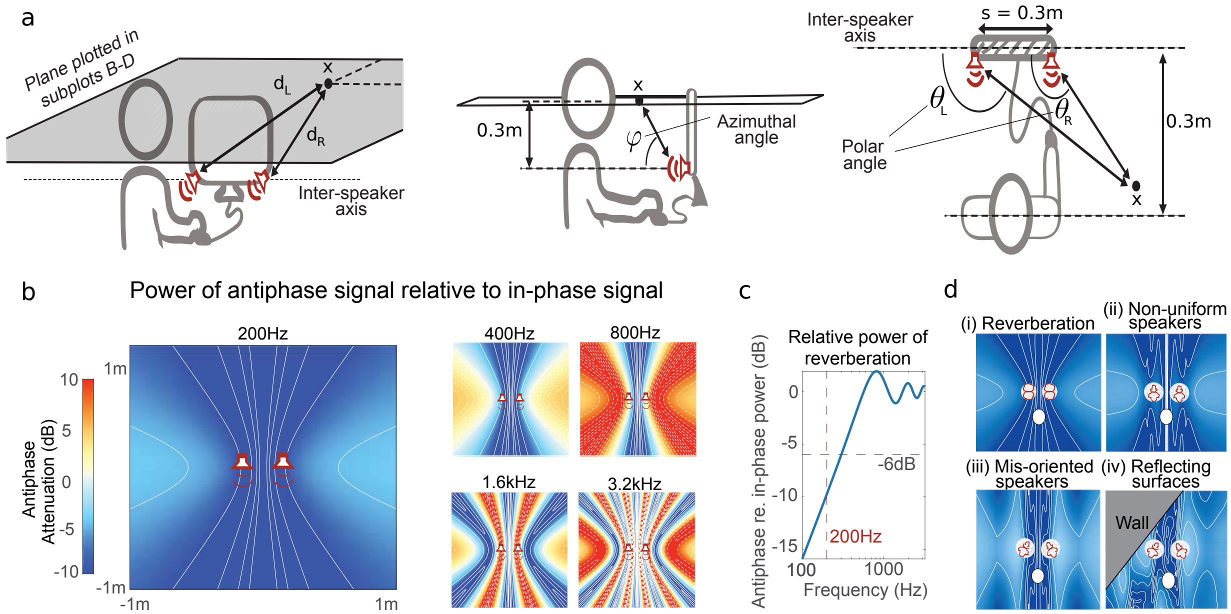

FIG. S1. Simulations of free-field attenuation. Simulations of free-field attenuation of tones broadcast in anti-phase relative to the same tones broadcast in-phase (i.e. the anti-phase attenuation) for a range of listening conditions. (a) Schematic of simulated listening setup and definition of coordinate system. The anti-phase attenuation at a point in space $\boldsymbol{x}$ depends upon the distance between that point and the left and right speakers (d_L and d_R, respectively). The simulations in B—D assume the speakers are separated by 30cm and we plot the attenuation in a horizontal plane 30cm above the speakers (the approximate location of a hypothetical listener's head). We use spherical polar coordinates referenced to the inter-speaker axis such that polar angle describes left-right variation and azimuthal angle describes forward-upward-backward-downward variation. (b) Reproduced from Fig.2A. Attenuation of anti-phase sinusoids from 200Hz-3.2kHz, in free-field listening conditions with uniformly radiating speakers. We plot the attenuation over a 2m x 2m region centered on the speakers. In all subsequent attenuation plots we show the same plane and use the same color scale. Solid contour lines indicate negative values and dashed contour lines indicate positive values. The technique works best at low frequencies, at which anti-phase signals are always attenuated. At higher frequencies the anti-phase signal is amplified in some locations. (c) Expected power of reverberation from anti-phase relative to in-phase broadcast as a function of tone frequency. The frequency we use (200Hz) and the level difference used in the task (-6dB) are marked by dashed lines. (d) Effect of (i) reverberation, (ii) non-uniform speaker radiation, (iii) mis-oriented speakers and (iv) reflections from a wall and table (not shown in figure) on anti-phase attenuation. In all cases the polar variation of the speakers are shown in inset plots over the speaker location (white circles depict 30dB range). The speakers simulated in (i) radiate uniformly, as in (b-c). The plotted values are integrated over azimuth. The polar variation apparent in (i) is due to the geometry of the coordinate system – when integrating over azimuth, the power broadcast between θ and $\theta + d\theta$ is proportional to $\sin\theta$. All simulations (i—iv) include reverberation.

A. Free-field attenuation

The parameter of importance for the screening task is the attenuation induced by the phase difference between stereo channels, which we term the anti-phase attenuation, given by

$$\Delta = 20\log_{10}\left(\frac{A_{\mathrm{total}}(\boldsymbol{x}, 180°)}{A_{\mathrm{total}}(\boldsymbol{x}, 0°)}\right) \tag{1}$$

where $A_{\mathrm{total}}(\boldsymbol{x}, \phi)$ is the signal amplitude, at point $\boldsymbol{x}$ in space, that results from broadcasting signals with a phase difference of ϕ between the right and left channels. Given that the two speaker channels are emitting sinusoids, the signal amplitude is given by the cosine rule:

$$A_{\mathrm{total}}^2(\boldsymbol{x}, \phi) = A_{\mathrm{L}}^2(\boldsymbol{x}) + A_{\mathrm{R}}^2(\boldsymbol{x}) + 2A_{\mathrm{L}}(\boldsymbol{x})A_{\mathrm{R}}(\boldsymbol{x})\cos\left(\phi + 2\pi\frac{(d_{\mathrm{L}} - d_{\mathrm{R}})}{\lambda}\right) \tag{2}$$

where $A_{\mathrm{L}}(\boldsymbol{x})$ and $A_{\mathrm{R}}(\boldsymbol{x})$ are the amplitudes of the signal from the left and right channels at $\boldsymbol{x}$, (this term thus accounts for the directionality of the speakers), d_{L} and d_{R} are the distances from the left and right speakers to $\boldsymbol{x}$, and λ is the wavelength of the signal.

For simplicity we first assume that the speakers radiate uniformly in all directions; we thus model the single-channel amplitudes by

$$A_{\mathrm{L}}(\boldsymbol{x}) = \frac{A_{\mathrm{L}}(\epsilon)}{\left({}^{d_{\mathrm{L}}}/_{\epsilon}\right)} \tag{3}$$

where $A_{\mathrm{L}}(\epsilon)$ is the broadcast level at distance ϵ from the speaker (i.e. just outside the speaker). This follows because acoustic power scales with the inverse square of distance (Jensen et al. 2000, Ch 2) and amplitude scales with the square-root of the power. $A_{\mathrm{R}}(\boldsymbol{x})$ is computed similarly with d_{L} in place of d_{R}. Note that both ϵ and $A_{\mathrm{L}}(\epsilon)$ cancel when substituted into Eq. (1).

There are two causes of phase difference between the sinusoidal tones broadcast from each speaker. The first is imposed deliberately, when we generate the anti-phase tones [i.e ϕ in Eq (2)]. The second is imposed by the spatial distance between the speakers and the location of the listener [i.e $\frac{d_{\mathrm{L}}-d_{\mathrm{R}}}{\lambda}$ in Eq. (2)]. For inter-speaker distances much smaller than one wavelength of the sinusoid, the second source of phase offset is negligible. Lower frequency tones thus allow attenuation with larger inter-speaker distances (because they have longer wavelengths). We accordingly used 200 Hz tones in our task.

We computed the anti-phase attenuation for tones from 200Hz – 3.2kHz assuming internal laptop speakers separated by 30cm. The results are shown in Fig. S1A-B in a plane 30cm above the laptop (i.e. the approximate location of a hypothetical listener's head). The results demonstrate that the method is more effective with low frequency tones; the higher frequency tones show narrower regions of destructive interference as well as regions of constructive interference. We identify three inter-speaker distance regimes (for reference, 200 Hz tones have a wavelength $\lambda{\sim}1.7m$), where s is the speaker separation:

1. $0 < s \leq \frac{\lambda}{4}$: Anti-phase tone attenuated everywhere (Fig. S1B; 200Hz).
2. $\frac{\lambda}{4} < s \leq \frac{\lambda}{2}$: Anti-phase tone attenuated everywhere except along the axis between the speakers, which is boosted; this is an unlikely listener location (Fig. S1B; 400Hz).

3. $\frac{\lambda}{2} < s < \infty$: Phase relationships complex, depend highly on specific location and scene; attenuation cannot be expected (Fig. S1B; >800Hz).

B. Effect of reverberation on anti-phase attenuation

The signal emitted by the speakers will reach the listener directly from the speakers as well as after reverberating in the space where the listener sits. Although the phase of individual paths taken by reverberant sound is randomized by interactions with the environment (Gardner, 2002; Traer and McDermott, 2016), anti-phase signals will nonetheless radiate less power due to interference. To quantify this effect, we estimate the power broadcast by the speaker pair to distances much greater than the separation distance between them, because reverberation is due to sounds that have reflected several times and may have propagated many meters. In this case we make the far-field assumption

$$\begin{aligned} (d_{\mathrm{L}} - d_{\mathrm{R}}) &\approx s\cos\theta \\ A_{\mathrm{L}}(\boldsymbol{x}) &\approx A_{\mathrm{R}}(\boldsymbol{x}) \end{aligned} \tag{4}$$

where s is the separation distance between the speakers and θ is the polar angle between the ray connecting the speaker to $\boldsymbol{x}$ and the inter-speaker axis connecting the speakers (Figure S1A). The amplitude at position $\boldsymbol{x}$ can be separated into contributions from radial distance, polar angle and azimuthal angle $A_{\mathrm{L}}(\boldsymbol{x}) = \alpha(r)\Theta(\theta)\Phi(\varphi)$ (and similarly for the right speaker). According to the far-field approximation the radial component (α) and the azimuthal component (Φ) will cancel when Eq. (2) is substituted into Eq. (1). We can thus compute the anti-phase attenuation from the angular components Θ_{L} and Θ_{R} only. The acoustic amplitude broadcast in a direction θ is thus given by a modified form of Eq (2)

$$\Theta_{\mathrm{total}}^2(\theta,\phi) = \Theta_{\mathrm{L}}^2(\theta) + \Theta_{\mathrm{R}}^2(\theta) + 2\Theta_{\mathrm{L}}(\theta)\Theta_{\mathrm{R}}(\theta)\cos\left(\phi + 2\pi\frac{s\cos\theta}{\lambda}\right) \tag{5}$$

From this, the directional amplitude can be computed for both in-phase and anti-phase signals. The total power emanating from the speakers (which is what determines the reverberant signal power) is given by integrating over all angles.

The effect of reverberation on the anti-phase attenuation (Δ) can be incorporated into the simulation of Fig. S1 by adding spatially uniform reverberating noise ρ to the simulated sound fields in phase and in anti-phase.

$$\Delta = 20\ \log_{10}\left(\frac{A_{\mathrm{total}}(\boldsymbol{x},180°) + }{A_{\mathrm{total}}(\boldsymbol{x},0°) + \ (0°)}\right) \tag{6}$$

Assuming an average reverberation 20dB lower than the direct signal arriving at the listener's ears (which is conservative for a source-listener distance of 30 cm) we can compute the reverberation from the two following relations

$$\rho(0°) + \rho(180°) = \frac{\left(A_{\mathrm{total}}(\boldsymbol{x}_{\mathrm{head}},0°) + A_{\mathrm{total}}(\boldsymbol{x}_{\mathrm{head}},180°)\right)}{10}$$

$$\frac{\rho(180°)}{\rho(0°)} = \frac{\int_0^{\pi} \Theta_{\mathrm{total}}\ (\theta,180°)\ \sin\theta\, \mathrm{d}\theta}{\int_0^{\pi} \Theta_{\mathrm{total}}\ (\theta,0°)\ \sin\theta\, \mathrm{d}\theta} \tag{7}$$

The effect of the anti-phase signal is to decrease the power of the reverberant energy by an amount that depends on the tone frequency (~10dB for the 200 Hz tone used in our experiments; Fig. S1C). This reverberation is included in the simulated anti-phase attenuation plots shown in Fig. S1D. It is apparent that the anti-phase attenuation persists with reverberation. Indeed, because the reverberant energy is spatially uniform, its effect is to reduce the spatial variation in the anti-phase attenuation, making the headphone check method more likely to work.

C. Effect of speaker directionality

We have thus far considered only speakers which broadcast uniformly in all directions, but this is unlikely to be the case with real speakers, which usually broadcast more energy directly from the front then from the sides or back. We model this explicitly by re-writing the single channel amplitude as

$$A_{\mathrm{L}}(r,\theta,\varphi) = \frac{\alpha_{\mathrm{L}}(\epsilon)}{\left({}^{d_{\mathrm{L}}}/_{\epsilon}\right)}\,\Theta_{\mathrm{L}}(\theta)\Phi_{\mathrm{L}}(\varphi) \tag{8}$$

where $\Theta(\theta)$ and $\Phi(\varphi)$ describe power variations with polar and azimuthal angle. We note that we use a spherical polar system referenced to the inter-speaker axis. Because the reference axis is horizontal – rather than vertical as is typical in discussions of binaural hearing – the polar angle θ describes left-to-right variation and the azimuthal angle φ describes forward-upward-backward-downward directional variation (Fig. S1A). An example attenuation map from directional speakers is shown (Fig. S1Dii) with polar and azimuthal power dependencies given by

$$\Theta_L(\theta) = 10^{\sin\theta\,|\sin(3\theta)|}$$

$$\Phi_L(\varphi) = 10^{\cos\varphi/2\,|\cos 4\varphi|} \tag{9}$$

These functions describe a speaker that broadcasts 20dB more power out the front than out the sides, 40dB more power out the front than the back, and which has multiple sidelobes around the peak value. The polar variation induces 2 sidelobes (Fig. S1Dii-iv; inset polar plots) to the right and left of center, and the azimuthal variation induces 3 sidelobes radiating from the top and 3 radiating from the bottom (not explicitly shown in the insets of Figure S1D). Although this example of directionality is arbitrary, it illustrates that the large-scale structure of the anti-phase attenuation shown in Fig. S1B is not particular to the special case of uniform radiation. We have simulated a wide range of speaker directionality functions and find that the anti-phase signal is consistently attenuated at all nearby locations irrespective of the specific details of the speaker. Using the same directional radiation functions, speakers that point in different directions can be simulated by substituting $\theta + \xi_{\mathrm{L}}$ and $\theta + \xi_{\mathrm{R}}$ into the speaker directionality functions [Eq. (9)] (Fig. S1Diii; $\xi_{\mathrm{L}} = \pi/4$, $\xi_{\mathrm{R}} = -\pi/4$). Once again the details of the attenuation map change but the attenuation at all locations around the speakers remains present.

D. Effect of nearby reflective surfaces

The near field can also be affected by reflections from nearby surfaces, which can be modeled by the method of images (Jensen et al, 2000, Ch 2)

$$A_{\mathrm{L}}(r,\theta,\varphi) = \frac{\alpha_{\mathrm{L}}(\epsilon)}{\left(d_{\mathrm{L}}/\epsilon\right)^2}\,\Theta_{\mathrm{L}}(\theta)\Phi_{\mathrm{L}}(\varphi) + \sum_{j=1}^{J}\frac{\Lambda_j\alpha_{\mathrm{L}}(\epsilon)}{\left(d_j/\epsilon\right)^2}\,\Theta_{\mathrm{L}}(\theta_j)\Phi_{\mathrm{L}}\left(\varphi_j\right) \tag{10}$$

where each reflecting surface (denoted by index j) induces an image source, the sound from which emanates from directions (θ_j, φ_j), is attenuated (by Λ_j, due to absorption) and propagates a distance d_j. Assuming the speakers rest 3cm above a table ($\Lambda_{\mathrm{table}} = 1$), 40cm from a single wall oriented at 45° to the interspeaker axis ($\Lambda_{\mathrm{table}} = 0.8$), the gross structure of the attenuation map (Fig. S1Div) remains similar to the other simulated cases.

These simulations (Fig. S1D) suggest that, for a reasonable range of scene and speaker parameters, anti-phase signals are likely to attenuate the level of a 200 Hz tone relative to in-phase 200 Hz tones.

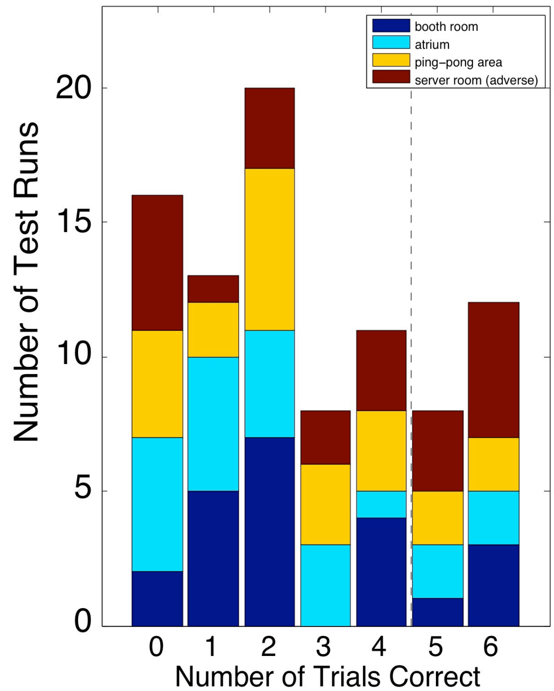

Fig. S2. In-lab screening task run through loudspeakers on participants' own laptops (Experiment 2), showing performance in the different testing rooms. Results from 88 test runs. Each of 22 participants performed the 6-trial screening task 4 times--once in each of 4 rooms (in random order).